Endometriotic Organoids as an *In Vitro* Model of Endometriotic Lesion Development.

Yong Song[1†], Gregory W. Burns[1†], Niraj R. Joshi[1], Ripla Arora[1], J. Julie Kim[2] and Asgerally T. Fazleabas[1*]

[1]Department of Obstetrics, Gynecology and Reproductive Biology, Michigan State University, Grand Rapids, MI 49503, USA

[2]Department of Obstetrics and Gynecology, Feinberg School of Medicine, Northwestern University, Chicago, IL, USA

[†]These authors contributed equally.

*Corresponding author. Email: fazleaba@msu.edu

One Sentence Summary:

Endometriotic organoids are an appropriate model to study epithelial-stromal interactions and model cell invasion associated with lesion development.

ABSTRACT

The development and progression of endometriotic lesions are poorly understood, but immune cell dysfunction and inflammation are closely associated with the pathophysiology of the disease. A lack of suitable 3D *in vitro* models permitting the study of interactions between cell types and the microenvironment is a contributing factor. To address this limitation, we developed endometriotic organoids (EO) to explore the role of epithelial-stromal interactions and model cell invasion associated with lesion development. Using a non-adherent microwell culture system, spherical organoids were generated with endometriotic epithelial cells (12Z) combined with immortalized endometriotic stromal cells (iEc-ESC) or immortalized uterine stromal cells (iHUF). Cell compartmentalization was observed in organoids with epithelial cells lining the periphery of a stromal cell core. Organoids with iEc-ESC (EO) stimulated the growth of a stratified epithelial cell layer compared to those with iHUF which developed a single layer. Transcriptome analysis found 4,522 differentially expressed genes (DEG) between organoid types and the top DEG included increased expression of interleukins and prostaglandin synthase enzymes. An overlap of the EO DEG with baboon endometriotic lesions was highly significant. Finally, to mimic invasion of endometrial tissue into the peritoneum, a model was developed using EO and an extracellular matrix containing human peritoneal mesothelial cells (LP9). Invasion of EO into the extracellular matrix-LP9 layer was increased in presence of estrogen or THP1-derived proinflammatory macrophages. Taken together, our results strongly support the concept that endometriotic organoids are an appropriate model for dissecting the mechanisms that contribute to endometriotic lesion development.

INTRODUCTION

Endometriosis is a chronic inflammatory hormone-dependent disorder which is characterized by the presence of endometrial tissue outside the uterus (1). It affects between 10 and 15% of all women of reproductive age, 70% of women with chronic pelvic pain, and 20–50% women with infertility (2, 3). The etiology and pathogenesis of endometriosis remains unclear, but lesion development has been associated with cellular proliferation and invasion, and interactions between endometriotic cells, immune cells and their microenvironment (4, 5). Appropriate *in vitro* platforms that allow dissection of the underlying mechanisms of these processes will inform the understanding of the disease and development of novel therapeutics.

Clinical samples from patients with endometriosis are the first line model to investigate the disease. One of the major limitations to understanding the pathological events associated with endometriosis is the significant delay of 8-11 years for diagnosis and subsequent variations in disease progression. Thus, both *in vivo* and *in vitro* models are indispensable to study the cellular and molecular mechanisms associated with endometriotic lesion development at different stages, The non-human primate and rodent models of endometriosis have been used most exclusively for *in vivo* studies. Non-human primates offer a physiologically relevant model and provide an opportunity to study both the early events and the disease progression (6, 7). Rodent models are advantageous due to the ability for tissue-specific gene manipulation and initial *in vivo* therapeutic testing(8). Most *in vitro* studies utilize two-dimensional monolayer culture of primary or immortalized endometrial cells. This method allows for the study of endometriosis associated mechanisms in a cell-specific manner and is easily manipulated for testing of treatments. However, the interactions are limited to the horizontal plane and cells are exposed to a uniform concentration of factors, so monolayer cultures are unable to mimic the architecture and function of tissues *in situ*. Thus, there is a significant gap between *in vivo* models and current *in vitro* cell culture techniques. Three-dimensional (3D) spheroids, or organoids, provide an exciting method to bridge the gap by incorporation of more complex structures and multiple cell types.

Organoids are self-organizing, genetically stable, 3D culture systems containing both

progenitor/stem and differentiated cells that resemble the tissue of origin (9-13). Boretto et al. first established endometriotic epithelial organoids in a Matrigel organoid culture system using ectopic lesions from patients with endometriosis and reported that the organoids replicated disease-associated functional and genomic traits (14). However, this system only allowed for the culture of endometriotic epithelial cells as stromal cells do not grow in these conditions. Wiwatpanit et al. generated endometrial organoids containing both epithelial and stromal cells from endometrial biopsies using micro-molded agarose plates and the scaffold-free organoids resembled the physiology of the native endometrium (13). The micro-molded agarose plate organoid culture system does not require exogenous scaffold materials but relies on *de novo* secretion of extracellular matrix and allows for self-organization and growth of multiple cell types.

An SV40-tranformed endometriotic epithelial cell line derived from peritoneal endometriosis, 12Z, is widely used for the study of endometriosis (15) and we recently developed an endometriotic stromal cell line (iEc-ESC) from ovarian endometriosis (16). In this study, our aim was to develop an endometriotic organoid model containing both endometriotic epithelial and stromal cell lines. We hypothesized that the transcriptome of scaffold-free organoids containing both endometriotic cell types would mirror endometriotic lesions from the baboon model and provide a model to explore peritoneal invasion associated with endometriotic lesion initiation.

RESULTS

Epithelial and Stromal Cells Self-Organize in Organoids

Epithelial and stromal cells are the two main cell types found in endometriotic lesions that are hypothesized to be descended from retrograde menstrual endometrial fragments. The cells employed in this study were immortalized ectopic epithelial cells (12Z), ectopic stromal cells (iEc-ESC) and human uterine fibroblasts (iHUF)(15, 16). For live visualization of cell-type organization, epithelial 12Z cells were modified to express red fluorescent protein (RFP) and both stromal cell lines to express Azurite blue. Endometrial organoids were generated from epithelial 12Z or stromal iEc-ESC alone, 12Z+iHUF, and 12Z+iEc-ESC in micro-molded agarose well plates. A preliminary study empirically determined that the optimal ratio of epithelial cells to stromal cells

for co-culture was 1:50. Time-lapse imaging demonstrated that epithelial and stromal cells reorganized autonomously in the agarose wells (Supplemental Video 1). The organization was confirmed by confocal imaging and Z-stack reconstruction, and immunohistochemical staining on days 4 and 7 (Fig 1). Organoids containing epithelial 12Z or stromal iEc-ESC alone formed solid spheroid structures at days 7 (Supplemental Fig 1). In contrast, when 12Z were co-cultured with iEc-ESC, a lesion-like structure was observed with organization of epithelial cells lining the periphery of stromal cells in the center of the spheroid at day 4 (Fig 1B). The observed morphology was very similar to endometrial organoids reported from primary cells (13).

We next sought to examine the effect of stromal cell origin on organoid formation by generating organoids with 12Z and iHUF or 12Z and iEc-ESC. Organoids containing iEc-ESC developed multiple epithelial cell layers while those containing normal stromal cells, iHUF, resulted in a single layer of epithelial cells at day 7 (Fig 1). This suggests that ectopic stromal cells promote epithelial cell proliferation and loss of apical-basal polarity and aligns with endometriotic epithelial stratification reported in Matrigel (14).

Endometriotic Organoids Invade a 3D Model of the Peritoneum

Cell invasion is one of the key processes involved in endometriotic lesion initiation and development. To simulate cell invasion that occurs *in vivo*, we developed a 3D endometriotic organoid invasion model. As shown in Fig 2A, human peritoneal mesothelial cells, LP9, expressing GFP were grown in Matrigel to mimic the structure of the peritoneum. Endometriotic organoids containing iEc-ESC and 12Z were seeded on the top of the LP9/Matrigel layer. The invasion of organoids was tracked using a fluorescent confocal microscopy every other day for 7 days. The Z-stack images were reconstructed to produce 3D models with Imaris image analysis software by Bitplane. As shown in Supplemental Video 2 and Fig 2C, the organoids invaded the Matrigel and continued penetrating the LP9 cell layer. Interestingly, stromal cells were always noted at the leading edge and as the first cell type to penetrate the LP9 cell layer, in alignment with previous observations (17, 18). These studies showed that endometrial stromal cells were the first cell type to attach and invade through the mesothelium in both nude mice and *ex vivo*

tissue explant cultures used to model the early stage of endometriosis (17, 18). The organoid invasion was quantified, and data are shown in Fig 2B. Combined, these results support the idea that the organoid invasion model could be an ideal *in vitro* tool to study the early events of endometriosis, particularly with respect to cell invasion.

Estrogen Stimulates Invasion of Endometriotic Organoids

Endometriosis is estrogen-dependent disease and estrogen can promote the migration and invasion of endometrial stromal cells and endometriotic epithelial cells in two-dimensional culture (19, 20). However, the effect of estrogen on organoids is unknown but we hypothesized that estradiol would stimulate invasion in our model. Invasion of Day 4 EO through the Matrigel/LP9 cell layer was monitored in the presence of 20nM estradiol (E2) or vehicle for 4 days. Organoids were imaged on Day 1 and Day 4 by fluorescent confocal microscopy. The invasion rate of endometriotic organoids was increased at 1.8-fold in the presence of E2 compared to vehicle ($p<0.05$; Fig 3).

Stromal Cell Origin Alters Organoid Gene Expression

We profiled the transcriptomes by RNA-sequencing of organoids containing ectopic stromal and epithelial cell lines (iEc-ESC/12Z; EO) and compared the profile to normal stromal and ectopic epithelial organoids (iHUF/12Z) to identify the global transcriptomic effect of ectopic stromal cells in the organoids. As an indication of broad transcriptome differences, EO and iHUF/12Z organoid samples were separated by principal component analysis across PC1 (65.7%, Fig 4A) and unsupervised hierarchical clustering (Fig 4B). Indeed, there were 4,522 differentially expressed genes (DEG), with 2,175 increased and 2,347 decreased, in EO compared to iHUF/12Z organoids. The top 50 DEG included increased expression of interleukins (*IL1B*, *IL24*), prostaglandin synthase enzymes (*PTGS1*, *PTGS2*), and telomerase reverse transcriptase (*TERT*). Of note, stromal cell lines were immortalized by constitutive expression of *TERT* via lentiviral transduction, but *TERT* was not differentially expressed in an analysis of organoids containing only stromal cells (Supplemental Fig 2), indicating the altered expression was due to an interaction between the epithelium and stroma cells.

Prostaglandin synthase enzymes, *PTGS1* and *PTGS2*, *CXCL8*, *TIMP3*, an inactivator of extracellular matrix remodeling enzymes, *IL1A*, and *LIF*, an estrogen response gene, were increased in EO while *STRA6* and *CRABP2*, retinoic acid binding proteins, and *PGR* were down-regulated (Fig 5A). Gene set enrichment analysis (GSEA) results included NFKB target genes, two senescence gene sets, and TNFα response via p38 mitogen-activated protein kinases as the most highly increased gene sets for EO, while stem cell-associated genes were decreased (Fig 5B).

Ectopic Organoids are Similar to Endometriotic Lesions

RNA-sequencing data from baboon endometrium and endometriotic lesions was compared to the human organoids and overlap of gene expression between these comparisons was highly significant, with 12,504 commonly expressed genes (Fig 6A). Additionally, GSEA using hallmark gene sets found similarities for comparisons of EO versus iHUF/12Z organoids and spontaneous baboon ectopic lesions versus eutopic endometrium (Fig 6B). TNF signaling via NFKB, inflammatory responses, and hypoxia associated genes were increased in EO and baboon lesions, while interferon alpha response was decreased in EO and increased in lesions. Similarly, allograft rejection and IL6 JAK/STAT3 signaling gene sets were increased in baboon ectopic lesions compared to eutopic tissues but absent from the organoid comparison. Gene ontology analysis of 2,518 genes identified only as expressed in baboon tissues resulted in significant enrichment for PANTHER GO-slim terms associated with the immune system (Table 1).

Proinflammatory Macrophages Increase Endometriotic Organoid Invasion

Immune cell dysfunction and local inflammation in the endometriotic environment have been considered to play a pivotal role in the pathogenesis of endometriosis (21). The recruitment of macrophages within the endometriotic lesion have been demonstrated to facilitate the development and maintenance of endometriosis (22-24). In support of a role for macrophages in the pathophysiology of endometriosis, immunoreactive CD68, a pan-macrophage marker, was detected in a baboon endometriotic lesion (Supplemental Fig 3). Proinflammatory, or M1, macrophages have the capacity to secrete inflammatory cytokines, including IL-6. These

172 inflammatory cytokines may further promote endometriotic cell growth and invasion (25). To
173 address the effect of activated proinflammatory macrophages on EO invasion, M1 were
174 differentiated from naïve (M0) macrophages derived from the THP1 cell line by exposure to IFN-
175 γ and lipopolysaccharide (LPS) for 24 hours. The resulting proinflammatory macrophages were
176 acclimatized for 24-36 hours in the organoid culture medium. As before, EO added to the top of
177 the Matrigel/LP9 layer and proinflammatory macrophages were added to the wells three hours
178 later. The EO were imaged on days 1 and 3 using fluorescent laser-scanning confocal microscopy.
179 Co-culture with either 7,500 or 15,000 macrophages increased EO invasion, while there was no
180 difference between the 7,500 and 15,000 macrophage treatment groups (Fig 7). Thus, the
181 addition of proinflammatory macrophages promoted the endometriotic organoid invasion in
182 support of the hypothesis that macrophages facilitate the establishment of endometriotic lesions.

183 **DISCUSSION**

184 A 3D organoid consisting of both epithelial and stromal cells makes an excellent model for
185 dissecting the mechanisms associated with early endometriotic lesion development *in vitro*. In this
186 study, we developed EO with endometriotic epithelial and stromal cell lines. The cells self-
187 organized and resulted in a stromal cell core surrounded by epithelial cells, a morphology is similar
188 to that of endometrial organoids derived from primary endometrial cells (13). Surprisingly, the
189 origin of the stromal cells, normal or ectopic altered the organoid structure with stratified epithelial
190 cells forming only with ectopic stromal cells. The observed epithelial stratification is consistent
191 with reports of endometriotic epithelial organoids grown in Matrigel (14). Transcriptomic analyses
192 revealed that known pathways dysregulated in endometriotic lesions were present in EO,
193 indicating that EO reproduce many hallmarks of the endometriosis-associated transcriptome.
194 Overall, our results support the idea that EO recapitulate the properties of endometriotic lesions
195 with respect to morphology, function, and gene expression.

196 Attachment and invasion are important steps in the development of endometriotic lesions (4).
197 Most current methods to study cell invasion are based on single cell types in 2D culture or
198 Transwell assays. To more accurately simulate the cell invasion process that occurs *in vivo*, we

199 developed a 3D organoid invasion model based on peritoneal endometriotic lesions. To our
200 knowledge, this is the first 3D invasion model which includes the three main cell compartments,
201 epithelial, stromal and peritoneal mesothelial cells. Endometriotic organoids migrated through a
202 layer of Matrigel, contacted, and penetrated through a layer of mesothelial cells, to mimic
203 peritoneal invasion. Interestingly, our results identified stromal cells at the leading edge of invasion
204 despite the structure of the organoid. This observation agrees with previous studies investigating
205 adhesion and invasion of endometrium to peritoneum using both nude mice and *ex vivo* tissue
206 explant culture models (17, 18). Endometrial stromal cells from women with endometriosis
207 undergo changes in adhesive properties and mesenchymal characteristics in response to
208 peritoneal mesothelial cells that might be part of the underlying mechanisms of lesion initiation
209 (26). Our data indicate that endometriotic organoids have the capacity to invade mesothelial cells
210 in a manner hypothesized to occur in physiological conditions. The utility of the organoid model
211 of invasion was further supported by increased invasive capacity in presence of estrogen or
212 activated proinflammatory macrophages. Collectively, this model expands the possibilities to
213 study mechanisms of endometriotic lesion establishment *in vitro*.

214 Stromal cell origin affected steroid hormone responsiveness of organoids and significantly
215 altered the transcriptome of endometriotic organoids with over 4,500 DEG. These observations
216 support the utility of a 3D organoid comprised of endometriotic epithelium and stroma. Indeed,
217 the genes expressed by EO largely mirrored those from spontaneous endometriotic lesions in the
218 baboon, and GSEA analyses confirmed coordinated increases in TNFα signaling via NFKB,
219 inflammatory responses, and hypoxia associated gene sets. Analysis of organoid gene
220 expression alterations associated with the origin of the stromal cells identified several pathways
221 known to be altered in endometriotic lesions, i.e., retinoic acid (RA) signaling that is altered in
222 endometriosis, both the uptake of retinoid (27) and the production of retinoic acid (RA) (28).
223 Several enzymes in the RA pathway were altered in endometriotic organoids, including decreased
224 expression of *STRA6* and *CRABP2* (29), and increased *CYP26B1*. Telomerase reverse
225 transcriptase (*TERT*) expression was increased in ectopic organoids, as *TERT* was amongst the

226 most highly upregulated genes but was not altered in a comparison of stroma-only organoids
227 (Supplemental Fig 2). There is significant evidence for increased expression of *TERT* in
228 endometriosis in eutopic secretory endometrium (30-34)and endometriotic lesions (35). In further
229 support of the model, endometriotic lesions are progestin resistant (36) and, concordantly,
230 progesterone receptor expression was downregulated in EO. The expression of leukemia
231 inhibitory factor (*LIF*) was increased in EO, possibly due to local estrogenic activity (37) or
232 inflammatory signals (38, 39). These results demonstrate significant alignment of the EO
233 transcriptome with spontaneous disease and specific pathways that are dysregulated in
234 endometriosis.

235 The immune system plays an important role in the establishment and progression of
236 endometriosis (25, 40, 41). Tissue resident immune cells are refluxed with menstrual tissue and
237 additional cells are recruited into the peritoneum where they interact with endometriotic lesions
238 (42). The pro-inflammatory cytokine *IL6* is common to all three coordinately increased hallmark
239 gene sets from EO and spontaneous endometriotic lesions from baboons (data not shown).
240 Interleukin-6 expression was increased in the spontaneous baboon lesions and EO and is
241 associated with chronic inflammation, endometriosis, and the presence of macrophages (22, 42-
242 44). IL-6 activates the expression of *CCL2* (also referred to as monocyte chemoattractant protein
243 1 or *MCP1*) in endothelial cells to recruit monocytes (45) and IL-6 is further produced by the
244 recruited macrophages and dendritic cells. Indeed, macrophages affect lesion establishment and
245 growth in a mouse model of endometriosis (22, 41, 42) and peritoneal macrophages from women
246 with endometriosis produce more IL-6 (46). Genes expressed in spontaneous lesions, but absent
247 from EO, were enriched in immune-related pathways indicating a role for immune cells in the
248 pathophysiology of endometriotic lesions that was absent in the model. Importantly, the invasive
249 capacity of EO was increased with the addition of proinflammatory macrophages, further
250 supporting this hypothesis. The mechanism by which the macrophages altered EO invasion is
251 undetermined, but IL-6 may be a key cytokine for the crosstalk between endometriotic lesions
252 and infiltrating macrophages.

253 The epithelial organoid culture system utilizing Matrigel supports extended culture of gland-
254 like epithelial structures but require expensive media components and does not allow for the
255 growth of stromal cells. Signaling between the epithelium and stromal compartments is critical for
256 normal functioning of the endometrium, both with respect to attainment of uterine receptivity and
257 embryo implantation (47, 48). Most cases of endometriosis are hypothesized to be the result of
258 retrograde menstruation of endometrial fragments containing both epithelium and stroma (49, 50).
259 Therefore, inclusion of both cell types more closely resembles the pathophysiology of
260 endometriosis and advances the potential for *in vitro* discovery. Ultra-low attachment plates and
261 hanging drop culture have been used recently to generate spheroids with 12Z cells, immortalized
262 stromal cells or primary ectopic stromal cells, or a combination of epithelial and stromal cells to
263 investigate endometriosis (51, 52). Interestingly, both culture models formed self-organizing
264 spheroid structures, but epithelial and stromal cell compartments were only evident in ultra-low
265 attachment conditions (51). Findings from our studies support the idea that 3D culture systems
266 allow for the study of complex cell interactions and invasion within a biologically relevant
267 microenvironment and are a promising new pre-clinical tool to evaluate therapeutic treatments for
268 endometriosis. Here, we describe scaffold-free self-organized endometriotic organoids,
269 comprised of both endometriotic epithelial and stromal cells combined with a novel model of
270 attachment and invasion of the peritoneum. Our results add to the support for *in vitro* 3D models
271 of endometriotic lesions to study mechanisms associated with the establishment endometriosis,
272 particularly with respect to cellular interactions and invasion. The EO recapitulated many of the
273 transcriptomic features of spontaneous peritoneal endometriotic lesions in the baboon and the
274 model allowed for real-time imaging and quantification of organoid invasion. The complexity of
275 this model could be increased by altering conditions with exogenous compounds or other cell
276 types. Future studies utilizing this system can capitalize on this flexibility with combinations of
277 additional cell types, individual cell type editing, and pharmacological compounds. Importantly,
278 our *in vitro* model does not reflect the full complexities of macrophage populations observed *in*
279 *vivo* (22, 41, 42). Experiments should investigate the interaction of peripheral monocytes or naïve

macrophages on EO and determine the effect on all cell types, including the resultant macrophage phenotypes. Furthermore, EO could also be integrated with microfluidics chips containing endometrium (53, 54) to study endometriosis associated endometrial receptivity failure and decidualization defects.

In conclusion, our study suggests that endometriotic organoids recapitulate the characteristics of endometriotic lesions and support the concept that endometriotic organoids are an appropriate model for dissecting the mechanisms that contribute to endometriotic lesion establishment.

MATERIALS AND METHODS

Cell Lines

Immortalized human ectopic endometriotic epithelial cells (12Z cells) (15) were cultured using Dulbecco's modified Eagle's medium (DMEM)/F-12 (Gibco, USA) supplemented with 10% Charcoal-dextran treated fetal bovine serum (CDS-FBS; Gibco, USA), 1X Pen/Strep (Gibco, USA) and 1X sodium pyruvate (Gibco, USA)(15, 55). The human peritoneal mesothelial cell line LP9 was kindly provided by Dr. James G. Rheinwald (Harvard Medical School, Boston, MA, USA). LP9 cells were maintained in a 1:1 ratio of M199 and Ham F12 media (Gibco), supplemented with 15% fetal bovine serum, 1% Penicillin/Streptomycin, 1% HEPES (Gibco), 1% GlutaMAX (Gibco), 10 ng/ml epidermal growth factor (EGF; Sigma, St Louis, MO, USA) and 400 ng/ml hydrocortisone (Sigma). The immortalized human endometriotic stromal cell line (iEc-ESC) was established in our laboratory(16). iEc-ESCs were cultured with phenol red–free DMEM/F12 medium supplemented with 10% charcoal dextran stripped fetal bovine serum (CDS-FBS), 100 units/ml of penicillin/streptomycin, and 1 mM sodium pyruvate. An immortalized human uterine fibroblast cell line (iHUF) was established from the decidua parietalis from term placenta in our laboratory. iHUF cells were cultured in phenol-red-free RPMI 1640 (Thermo Fisher Scientific) supplemented with 10% CDS-FBS, 100 units/ml of penicillin/streptomycin, and 1 mM sodium pyruvate. THP1 cells (kindly provided by Dr. Margaret Petroff, Michigan State University) were grown in T75 flask using RPMI1640 with 10% FBS in the presence of Antibiotic-Antimycotic in the suspension culture.

These cells were sub-cultured either in 6-well plates or T-25 flask and treated with 100nM (1:5000 µl of media) PMA (Phorbo 12-Myristate 13-Acetate, Cayman Chemicals, USA) to yield 60-70% adherent cells at the end of 24 hours. The PMA exposure was repeated, and any floating non-confluent cells were removed. The cell obtained following PMA treatment were designated as M0 macrophages and kept in pre-differentiated (M0) state for 2-4 days before exposing them to M1/ M2 differentiation. These M0 adherent macrophages were activated with 20 ng/ml IFN-gamma (R&D Systems, USA) and 10pg/ ml of LPS (Sigma, USA.) for 24 hours to differentiate into M1 proinflammatory macrophages utilized to study effect of proinflammatory M1 macrophage on endometriotic organoid culture system. All cell lines were maintained at 37ºC in an atmosphere of 5% CO_2 in air.

RFP lentiviral vector (Ploc-RFP) was used to generate fluorescently tagged 12Z-RFP cell line. EGFP lentiviral vector (pHX-EGFP) was utilized to generate LP9-GFP stable cell lines. iEC-ESCs and iHUF cells were tagged with Azurite blue using pLV-Azurite (Addgene plasmid 36086). Lentiviral transductions were performed according to manufacturers' protocols and successfully tagged cells were further sorted on a Beckman Coulter MoFlow Astrios (Indianapolis, IN, USA).

Generation of Endometriotic Organoids

12Z and stromal cells were trypsinized in the flask and cell suspensions were centrifuged at 200 x*g* for 5 minutes. Both epithelial and stromal cell pellets were then suspended in complete MammoCult human medium (STEMCELL Technologies, Inc., 05620) supplemented with hydrocortisone and heparin as per the manufacturer's instructions and 1% pen/strep (Sigma, P0781) to similar densities. Epithelial and stromal cells were mixed at a 1:50 ratio by volume and 50uL of epithelial-stromal cell suspension was seeded into 1.5% (w/v) agarose 3D micro-molded plate, prepared according to the manufacturer's instructions (MicroTissues® 3D Petri Dish® micro-mold spheroids, Sigma, Z764043). Cells were cultured in MammoCult growth medium for at least 4 days to allow organoid formation prior to further treatment. Media was changed every 2-3 days.

Organoid Invasion Model

To mimic the structure of the peritoneum, an ice cold LP9 cell suspension was mixed with ice cold Matrigel (Corning, 536232) at a ratio of 2:1(v:v), 30ul drops of Matrigel-cell suspension were plated into 96-well plate, at a density of 2-2.5x10^4 cells per well, allowed to set at 37℃ for 3-4 hours until solidified and overlaid with 100ul MammoCult growth medium. The next day, the day 4 endometriotic organoids were harvested from 3D Petri Dishes® by pipetting and then seeded on to the top of Matrigel-LP9-GFP layer in 96-well plates in 100ul MammoCult growth medium. Organoid invasion into the LP9-GFP/Matrigel layer were imaged every 48 hours using confocal microscopy.

Organoid Imaging

Organoids were imaged using a Nikon Eclipse Ti inverted microscope using a Nikon C2 + confocal microscope laser scanner. For each organoid, z-stacks were generated with a 10μm increment, and tiled scans were set up to image the entire width and depth of the organoid with 10x air objective. The position of the each organoid was recorded as x,y coordinate by ND Acquisition of NIS-Elements software. For organoid sections, z-stacks were generated with 0.5μm increment using 40X oil objective. Images were merged using NIS-Elements C2 version 4.13.

Quantification of Invasion

Commercial software Imaris x64 7.4.2 (Bitplane) was used for image analysis. In order to quantify the invasion of the organoid stromal cells into the peritoneal mesothelial cells, 3D surface models of the LP9-GFP cell layer, and the stromal cells-Azurite blue were created. Using the measurement function in Imaris, and using orthogonal slicers in XY, YZ and ZX planes, the linear distance between the organoid tip and the organoid migrating front on to the peritoneal cells were calculated. The distances were calculated at different time points in order to calculate velocity of organoid movement as a function of time. Seven to ten organoids for each time point in different groups were evaluated to account for heterogeneity in organoid structure as well as movement.

Immunofluorescence Staining

Agarose 3D Petri Dishes® containing organoids were removed from the tissue culture plate

361 and the medium inside was removed gently by pipetting under a dissecting microscope.
362 Organoids were sealed within the agarose dish with lukewarm 1.5% (w/v) agarose in 1×PBS. The
363 sealed 3D Petri Dishes® containing organoids were then fixed in 4% paraformaldehyde in 1×PBS
364 at 4°C overnight, rinsed briefly in 1×PBS, stored in 70% EtOH and processed for standard paraffin
365 embedding and sectioning at 6μm. Organoid sections were dewaxed, and then rehydrated with a
366 graded alcohol series, followed by heat-mediated antigen retrieval in citrate buffer (Vector
367 Laboratories, H3300) and then hydrogen peroxide treatment. Sections were blocked for 1 h in 10%
368 normal horse serum (Vector Laboratories, S-2000) in PBS and incubated overnight at 4°C in
369 primary antibodies. Organoid sections were incubated in respective species specific
370 fluorochrome-conjugated secondary antibodies following an overnight incubation with the primary
371 antibodies. Slides were then mounted with Antifade Mounting Medium with DAPI (Vector
372 Laboratories, H-1200). Images were captured with a Nikon Eclipse Ti inverted microscope using
373 software from NIS Elements, Inc. (Nikon, Melville, NY). The primary antibodies used were
374 Vimentin polyclonal antibody (5741S) from Cell Signaling Technology, Inc. (Waltham, MA).
375 Cytokeratin, pan (mixture) monoclonal antibody (C2562), from Sigma-Aldrich (St. Louis, MO). The
376 secondary antibodies were: DyLight 594 goat anti-rabbit IgG antibody (DI-1594) from Vector
377 Laboratories (Burlingame, CA). Alexa Fluor® 488 AffiniPure donkey anti-mouse IgG (715-545-
378 150) from Jackson ImmunoResearch Laboratories Inc. (West Grove, PA).

379 **RNA-sequencing and Data Analysis**

380 For RNA-sequencing, the Arcturus PicoPure RNA Isolation Kit (Themo Fisher Scientific,
381 12204-01), including an on-column DNA digestion using the RNAse-free DNAse set (Qiagen;
382 79254), was used to purify RNA from whole organoids. Total RNA was isolated from snap-frozen
383 tissues homogenized in TRIzol reagent (Thermo Fisher; 15596018) following the manufacturer's
384 instructions. RNA was stored at -80°C in nuclease-free water and concentration was determined
385 with a Nanodrop 1000 instrument (Thermo Fisher Scientific). Samples were sent to a sequencing
386 facility (Novogene Corporation Inc., Chula Vista, CA) for RNA integrity analysis, library preparation,
387 and sequencing. Libraries were prepared with an TruSeq mRNA kit (Illumina Inc., San Diego, CA)

and sequenced (paired end 150 bp) on a NovaSeq 6000 instrument (Illumina Inc.) to an average depth of 39 million fragments per sample. Reads were quality trimmed and adapters were removed using TrimGalore (version 0.6.5) (56), and quality trimmed reads were assessed with FastQC (version 0.11.7). Trimmed reads were mapped to *Homo sapiens* genome assembly GRCh38 (hg38) or *Papio anubis* (version 3.0) using using HISAT2 (version 2.0.3) (57). Reads overlapping Ensembl annotations (version 99) (58) were quantified with featureCounts (version 1.6.2) (59) prior to model-based differential expression (DE) analysis using the edgeR-robust method (version 4.0.3) (60) in R. Genes with low counts per million (CPM) were removed using the filterByExpr function from edgeR. Transcriptome-wide read distributions were plotted to ensure a similar distribution across all samples with boxplots of log-transformed CPM values. Multidimensional scaling plots, generated with the plotMDS function of edgeR, were used to verify group separation prior to statistical analysis. Principal component analysis of normalized counts was conducted with the prcomp function in R using the top 500 variable genes. Differentially expressed genes (DEG) were identified as false discovery rate (FDR) p-value less than 0.05.

The hclust package was used for hierarchical clustering (ward.D) of Euclidean distances. Heat maps were generated using log-transformed transcript per million values (TPM) in pheatmap (version 1.0.12). Where necessary, baboon Ensembl genes were converted to human entrez identifiers with the human ortholog table downloaded from Biomart (version 101). The phyper function in R was used for hypergeometric tests of overlapping genes. Gene set enrichment and over-representation analyses were completed with clusterProfiler package (version 3.16.1) using mSigDB and KEGG reference databases.

Statistical Analysis

Unless otherwise stated, statistical analysis was performed using GraphPad Prism 9.00 (GraphPad). All data were expressed as mean ± SD. The Student's t test was used for comparisons between the 2 groups, and 1-way ANOVA with a post hoc test least-significant difference was used for multiple comparisons. $P < 0.05$ was considered statistically significant (2-tailed).

LIST OF SUPPLEMENTARY MATERIALS

Fig. S1. Epithelial and stromal cell organization in organoid culture.

Fig. S2. Telomerase reverse transcriptase (TERT) expression in organoids.

Fig. S3. Macrophages are present in baboon endometriotic lesions.

Movie S1. Endometriotic organoids self-organize into epithelium and stroma compartments.

Movie S2. Confocal live imaging of EO invasion through a mesothelial cell layer over 8 days.

REFERENCES

1. Giudice LC. Clinical practice. Endometriosis. N Engl J Med. 2010;362(25):2389-98. Epub 2010/06/25. doi: 10.1056/NEJMcp1000274. PubMed PMID: 20573927; PMCID: PMC3108065.
2. Practice Committee of the American Society for Reproductive Medicine. Treatment of pelvic pain associated with endometriosis. Fertil Steril. 2008;90(5 Suppl):S260-9. Epub 2008/11/26. doi: 10.1016/j.fertnstert.2008.08.057. PubMed PMID: 19007642.
3. Endometriosis and infertility: a committee opinion. Fertil Steril. 2012;98(3):591-8. Epub 2012/06/19. doi: 10.1016/j.fertnstert.2012.05.031. PubMed PMID: 22704630.
4. Burney RO, Giudice LC. Pathogenesis and pathophysiology of endometriosis. Fertil Steril. 2012;98(3):511-9. Epub 2012/07/24. doi: 10.1016/j.fertnstert.2012.06.029. PubMed PMID: 22819144.
5. Yang HL, Zhou WJ, Chang KK, Mei J, Huang LQ, Wang MY, Meng Y, Ha SY, Li DJ, Li MQ. The crosstalk between endometrial stromal cells and macrophages impairs cytotoxicity of NK cells in endometriosis by secreting IL-10 and TGF-β. Reproduction. 2017;154(6):815-25. Epub 2017/10/04. doi: 10.1530/rep-17-0342. PubMed PMID: 28971893.
6. Fazleabas AT. A baboon model for inducing endometriosis. Methods Mol Med. 2006;121:95-9. Epub 2005/10/28. PubMed PMID: 16251737.
7. Harirchian P, Gashaw I, Lipskind ST, Braundmeier AG, Hastings JM, Olson MR, Fazleabas AT. Lesion kinetics in a non-human primate model of endometriosis. Hum Reprod. 2012;27(8):2341-51. Epub 2012/06/08. doi: 10.1093/humrep/des196. PubMed PMID: 22674203; PMCID: PMC3398680.
8. Bruner-Tran KL, Mokshagundam S, Herington JL, Ding T, Osteen KG. Rodent Models of Experimental Endometriosis: Identifying Mechanisms of Disease and Therapeutic Targets. Curr Womens Health Rev. 2018;14(2):173-88. Epub 2018/06/05. doi: 10.2174/1573404813666170921162041. PubMed PMID: 29861705; PMCID: PMC5925870.
9. Schutgens F, Verhaar MC, Rookmaaker MB. Pluripotent stem cell-derived kidney organoids: An in vivo-like in vitro technology. Eur J Pharmacol. 2016;790:12-20. Epub 2016/07/05. doi: 10.1016/j.ejphar.2016.06.059. PubMed PMID: 27375081.
10. Leibel SL, McVicar RN, Winquist AM, Niles WD, Snyder EY. Generation of Complete Multi-Cell Type Lung Organoids From Human Embryonic and Patient-Specific Induced Pluripotent Stem Cells for Infectious Disease Modeling and Therapeutics Validation. Curr Protoc Stem Cell Biol. 2020;54(1):e118. Epub 2020/07/09. doi: 10.1002/cpsc.118. PubMed PMID: 32640120; PMCID: PMC7361156.
11. Boretto M, Cox B, Noben M, Hendriks N, Fassbender A, Roose H, Amant F, Timmerman D, Tomassetti C, Vanhie A, Meuleman C, Ferrante M, Vankelecom H. Development of organoids from mouse and human endometrium showing endometrial epithelium physiology and long-term expandability. Development. 2017;144(10):1775-86. Epub 2017/04/27. doi: 10.1242/dev.148478. PubMed PMID: 28442471.
12. Turco MY, Gardner L, Hughes J, Cindrova-Davies T, Gomez MJ, Farrell L, Hollinshead M, Marsh SGE, Brosens JJ, Critchley HO, Simons BD, Hemberger M, Koo BK, Moffett A, Burton GJ.

462 Long-term, hormone-responsive organoid cultures of human endometrium in a chemically defined
463 medium. Nat Cell Biol. 2017;19(5):568-77. Epub 2017/04/11. doi: 10.1038/ncb3516. PubMed
464 PMID: 28394884; PMCID: PMC5410172.
465 13. Wiwatpanit T, Murphy AR, Lu Z, Urbanek M, Burdette JE, Woodruff TK, Kim JJ. Scaffold-Free
466 Endometrial Organoids Respond to Excess Androgens Associated With Polycystic Ovarian
467 Syndrome. J Clin Endocrinol Metab. 2020;105(3). Epub 2019/10/16. doi: 10.1210/clinem/dgz100.
468 PubMed PMID: 31614364; PMCID: PMC7112974.
469 14. Boretto M, Maenhoudt N, Luo X, Hennes A, Boeckx B, Bui B, Heremans R, Perneel L,
470 Kobayashi H, Van Zundert I, Brems H, Cox B, Ferrante M, Uji IH, Koh KP, D'Hooghe T, Vanhie A,
471 Vergote I, Meuleman C, Tomassetti C, Lambrechts D, Vriens J, Timmerman D, Vankelecom H.
472 Patient-derived organoids from endometrial disease capture clinical heterogeneity and are
473 amenable to drug screening. Nat Cell Biol. 2019;21(8):1041-51. Epub 2019/08/03. doi:
474 10.1038/s41556-019-0360-z. PubMed PMID: 31371824.
475 15. Zeitvogel A, Baumann R, Starzinski-Powitz A. Identification of an invasive, N-cadherin-
476 expressing epithelial cell type in endometriosis using a new cell culture model. Am J Pathol.
477 2001;159(5):1839-52. Epub 2001/11/07. doi: 10.1016/S0002-9440(10)63030-1. PubMed PMID:
478 11696444; PMCID: PMC1867070.
479 16. Song Y, Joshi NR, Vegter E, Hrbek S, Lessey BA, Fazleabas AT. Establishment of an
480 Immortalized Endometriotic Stromal Cell Line from Human Ovarian Endometrioma. Reproductive
481 sciences (Thousand Oaks, Calif). 2020. Epub 2020/06/17. doi: 10.1007/s43032-020-00228-0.
482 PubMed PMID: 32542539.
483 17. Witz CA, Monotoya-Rodriguez IA, Schenken RS. Whole explants of peritoneum and
484 endometrium: a novel model of the early endometriosis lesion. Fertil Steril. 1999;71(1):56-60.
485 Epub 1999/02/06. doi: 10.1016/s0015-0282(98)00400-2. PubMed PMID: 9935116.
486 18. Nisolle M, Casanas-Roux F, Donnez J. Early-stage endometriosis: adhesion and growth of
487 human menstrual endometrium in nude mice. Fertil Steril. 2000;74(2):306-12. Epub 2000/08/06.
488 PubMed PMID: 10927049.
489 19. Xiong W, Zhang L, Yu L, Xie W, Man Y, Xiong Y, Liu H, Liu Y. Estradiol promotes cells invasion
490 by activating β-catenin signaling pathway in endometriosis. Reproduction. 2015;150(6):507-16.
491 Epub 2015/10/04. doi: 10.1530/rep-15-0371. PubMed PMID: 26432349; PMCID: PMC4633770.
492 20. Du Y, Zhang Z, Xiong W, Li N, Liu H, He H, Li Q, Liu Y, Zhang L. Estradiol promotes EMT in
493 endometriosis via MALAT1/miR200s sponge function. Reproduction. 2019;157(2):179-88. Epub
494 2018/12/01. doi: 10.1530/rep-18-0424. PubMed PMID: 30500775; PMCID: PMC7305834.
495 21. Ahn SH, Monsanto SP, Miller C, Singh SS, Thomas R, Tayade C. Pathophysiology and
496 Immune Dysfunction in Endometriosis. Biomed Res Int. 2015;2015:795976. Epub 2015/08/08.
497 doi: 10.1155/2015/795976. PubMed PMID: 26247027; PMCID: PMC4515278.
498 22. Bacci M, Capobianco A, Monno A, Cottone L, Di Puppo F, Camisa B, Mariani M, Brignole C,
499 Ponzoni M, Ferrari S, Panina-Bordignon P, Manfredi AA, Rovere-Querini P. Macrophages are
500 alternatively activated in patients with endometriosis and required for growth and vascularization
501 of lesions in a mouse model of disease. Am J Pathol. 2009;175(2):547-56. Epub 2009/07/04. doi:
502 10.2353/ajpath.2009.081011. PubMed PMID: 19574425; PMCID: PMC2716955.

503 23. Haber E, Danenberg HD, Koroukhov N, Ron-El R, Golomb G, Schachter M. Peritoneal
504 macrophage depletion by liposomal bisphosphonate attenuates endometriosis in the rat model.
505 Hum Reprod. 2009;24(2):398-407. Epub 2008/10/25. doi: 10.1093/humrep/den375. PubMed
506 PMID: 18948309.
507 24. Vercellini P, Vigano P, Somigliana E, Fedele L. Endometriosis: pathogenesis and treatment.
508 Nat Rev Endocrinol. 2014;10(5):261-75. Epub 2013/12/25. doi: 10.1038/nrendo.2013.255.
509 PubMed PMID: 24366116.
510 25. Izumi G, Koga K, Takamura M, Makabe T, Satake E, Takeuchi A, Taguchi A, Urata Y, Fujii T,
511 Osuga Y. Involvement of immune cells in the pathogenesis of endometriosis. J Obstet Gynaecol
512 Res. 2018;44(2):191-8. Epub 2018/01/10. doi: 10.1111/jog.13559. PubMed PMID: 29316073.
513 26. Lin LL, Makwana S, Chen M, Wang CM, Gillette LH, Huang TH, Burney RO, Nicholson BJ,
514 Kirma NB. Cellular junction and mesenchymal factors delineate an endometriosis-specific
515 response of endometrial stromal cells to the mesothelium. Mol Cell Endocrinol. 2021;539:111481.
516 Epub 2021/10/09. doi: 10.1016/j.mce.2021.111481. PubMed PMID: 34624439.
517 27. Pavone ME, Reierstad S, Sun H, Milad M, Bulun SE, Cheng YH. Altered retinoid uptake and
518 action contributes to cell survival in endometriosis. J Clin Endocrinol Metab. 2010;95(11):E300-9.
519 Epub 2010/08/13. doi: 10.1210/jc.2010-0459. PubMed PMID: 20702525; PMCID: PMC2968735.
520 28. Pierzchalski K, Taylor RN, Nezhat C, Jones JW, Napoli JL, Yang G, Kane MA, Sidell N.
521 Retinoic acid biosynthesis is impaired in human and murine endometriosis. Biol Reprod.
522 2014;91(4):84. Epub 2014/08/22. doi: 10.1095/biolreprod.114.119677. PubMed PMID: 25143356;
523 PMCID: PMC4435029.
524 29. Pavone ME, Grover AR, Confino R, Pearson EK, Malpani S, Cheng Y-H, Fazleabas A, Bulun
525 S. Retinoic acid action is altered within endometrium of baboons affected with endometriosis.
526 Journal of Endometriosis and Pelvic Pain Disorders. 2022. doi: 10.1177/22840265211062008.
527 30. Kim CM, Oh YJ, Cho SH, Chung DJ, Hwang JY, Park KH, Cho DJ, Choi YM, Lee BS.
528 Increased telomerase activity and human telomerase reverse transcriptase mRNA expression in
529 the endometrium of patients with endometriosis. Hum Reprod. 2007;22(3):843-9. Epub
530 2006/11/02. doi: 10.1093/humrep/del425. PubMed PMID: 17077107.
531 31. Hapangama DK, Turner MA, Drury JA, Quenby S, Saretzki G, Martin-Ruiz C, Von Zglinicki T.
532 Endometriosis is associated with aberrant endometrial expression of telomerase and increased
533 telomere length. Hum Reprod. 2008;23(7):1511-9. Epub 2008/05/06. doi:
534 10.1093/humrep/den172. PubMed PMID: 18456668.
535 32. Valentijn AJ, Palial K, Al-Lamee H, Tempest N, Drury J, Von Zglinicki T, Saretzki G, Murray P,
536 Gargett CE, Hapangama DK. SSEA-1 isolates human endometrial basal glandular epithelial cells:
537 phenotypic and functional characterization and implications in the pathogenesis of endometriosis.
538 Hum Reprod. 2013;28(10):2695-708. Epub 2013/07/13. doi: 10.1093/humrep/det285. PubMed
539 PMID: 23847113.
540 33. Mafra FA, Christofolini DM, Cavalcanti V, Vilarino FL, André GM, Kato P, Bianco B, Barbosa
541 CP. Aberrant telomerase expression in the endometrium of infertile women with deep
542 endometriosis. Arch Med Res. 2014;45(1):31-5. Epub 2013/12/11. doi:
543 10.1016/j.arcmed.2013.12.002. PubMed PMID: 24321595.

34. Hapangama DK, Kamal A, Saretzki G. Implications of telomeres and telomerase in endometrial pathology. Hum Reprod Update. 2017;23(2):166-87. Epub 2016/12/17. doi: 10.1093/humupd/dmw044. PubMed PMID: 27979878; PMCID: PMC5850744.
35. Hapangama DK, Turner MA, Drury J, Heathcote L, Afshar Y, Mavrogianis PA, Fazleabas AT. Aberrant expression of regulators of cell-fate found in eutopic endometrium is found in matched ectopic endometrium among women and in a baboon model of endometriosis. Hum Reprod. 2010;25(11):2840-50. Epub 2010/09/23. doi: 10.1093/humrep/deq248. PubMed PMID: 20858696; PMCID: PMC2955559.
36. Attia GR, Zeitoun K, Edwards D, Johns A, Carr BR, Bulun SE. Progesterone receptor isoform A but not B is expressed in endometriosis. J Clin Endocrinol Metab. 2000;85(8):2897-902. Epub 2000/08/18. doi: 10.1210/jcem.85.8.6739. PubMed PMID: 10946900.
37. Bulun SE, Yang S, Fang Z, Gurates B, Tamura M, Sebastian S. Estrogen production and metabolism in endometriosis. Annals of the New York Academy of Sciences. 2002;955:75-85; discussion 6-8, 396-406. Epub 2002/04/13. doi: 10.1111/j.1749-6632.2002.tb02767.x. PubMed PMID: 11949967.
38. Knight D. Leukaemia inhibitory factor (LIF): a cytokine of emerging importance in chronic airway inflammation. Pulm Pharmacol Ther. 2001;14(3):169-76. Epub 2001/07/13. doi: 10.1006/pupt.2001.0282. PubMed PMID: 11448143.
39. Rosario GX, Stewart CL. The Multifaceted Actions of Leukaemia Inhibitory Factor in Mediating Uterine Receptivity and Embryo Implantation. Am J Reprod Immunol. 2016;75(3):246-55. Epub 2016/01/29. doi: 10.1111/aji.12474. PubMed PMID: 26817565.
40. Lebovic DI, Mueller MD, Taylor RN. Immunobiology of endometriosis. Fertil Steril. 2001;75(1):1-10. Epub 2001/02/13. doi: 10.1016/s0015-0282(00)01630-7. PubMed PMID: 11163805.
41. Hogg C, Horne AW, Greaves E. Endometriosis-Associated Macrophages: Origin, Phenotype, and Function. Front Endocrinol (Lausanne). 2020;11:7. Epub 2020/02/11. doi: 10.3389/fendo.2020.00007. PubMed PMID: 32038499; PMCID: PMC6989423.
42. Hogg C, Panir K, Dhami P, Rosser M, Mack M, Soong D, Pollard JW, Jenkins SJ, Horne AW, Greaves E. Macrophages inhibit and enhance endometriosis depending on their origin. Proc Natl Acad Sci U S A. 2021;118(6). Epub 2021/02/05. doi: 10.1073/pnas.2013776118. PubMed PMID: 33536334.
43. Gabay C. Interleukin-6 and chronic inflammation. Arthritis Res Ther. 2006;8 Suppl 2(Suppl 2):S3. Epub 2006/08/11. doi: 10.1186/ar1917. PubMed PMID: 16899107; PMCID: PMC3226076.
44. Capobianco A, Monno A, Cottone L, Venneri MA, Biziato D, Di Puppo F, Ferrari S, De Palma M, Manfredi AA, Rovere-Querini P. Proangiogenic Tie2(+) macrophages infiltrate human and murine endometriotic lesions and dictate their growth in a mouse model of the disease. Am J Pathol. 2011;179(5):2651-9. Epub 2011/09/20. doi: 10.1016/j.ajpath.2011.07.029. PubMed PMID: 21924227; PMCID: PMC3204092.
45. Romano M, Sironi M, Toniatti C, Polentarutti N, Fruscella P, Ghezzi P, Faggioni R, Luini W, van Hinsbergh V, Sozzani S, Bussolino F, Poli V, Ciliberto G, Mantovani A. Role of IL-6 and its soluble receptor in induction of chemokines and leukocyte recruitment. Immunity. 1997;6(3):315-

585 25. Epub 1997/03/01. doi: 10.1016/s1074-7613(00)80334-9. PubMed PMID: 9075932.
586 46. Montagna P, Capellino S, Villaggio B, Remorgida V, Ragni N, Cutolo M, Ferrero S. Peritoneal
587 fluid macrophages in endometriosis: correlation between the expression of estrogen receptors
588 and inflammation. Fertil Steril. 2008;90(1):156-64. Epub 2007/06/06. doi:
589 10.1016/j.fertnstert.2006.11.200. PubMed PMID: 17548071.
590 47. Wetendorf M, DeMayo FJ. Progesterone receptor signaling in the initiation of pregnancy and
591 preservation of a healthy uterus. Int J Dev Biol. 2014;58(2-4):95-106. Epub 2014/07/16. doi:
592 10.1387/ijdb.140069mw. PubMed PMID: 25023675; PMCID: PMC4413906.
593 48. Wang X, Wu SP, DeMayo FJ. Hormone dependent uterine epithelial-stromal communication
594 for pregnancy support. Placenta. 2017;60 Suppl 1:S20-S6. Epub 2017/07/19. doi:
595 10.1016/j.placenta.2017.07.003. PubMed PMID: 28716426; PMCID: PMC5743625.
596 49. Sampson JA. Peritoneal endometriosis due to the menstrual dissemination of endometrial
597 tissue into the peritoneal cavity. American Journal of Obstetrics & Gynecology. 1927;14(4):422-
598 69. doi: 10.1016/S0002-9378(15)30003-X.
599 50. Zondervan KT, Becker CM, Koga K, Missmer SA, Taylor RN, Vigano P. Endometriosis. Nat
600 Rev Dis Primers. 2018;4(1):9. Epub 2018/07/22. doi: 10.1038/s41572-018-0008-5. PubMed
601 PMID: 30026507.
602 51. Wendel JRH, Wang X, Smith LJ, Hawkins SM. Three-Dimensional Biofabrication Models of
603 Endometriosis and the Endometriotic Microenvironment. Biomedicines. 2020;8(11). Epub
604 2020/11/26. doi: 10.3390/biomedicines8110525. PubMed PMID: 33233463.
605 52. Stejskalova A, Fincke V, Nowak M, Schmidt Y, Borrmann K, von Wahlde MK, Schafer SD,
606 Kiesel L, Greve B, Gotte M. Collagen I triggers directional migration, invasion and matrix
607 remodeling of stroma cells in a 3D spheroid model of endometriosis. Sci Rep. 2021;11(1):4115.
608 Epub 2021/02/20. doi: 10.1038/s41598-021-83645-8. PubMed PMID: 33603041; PMCID:
609 PMC7892880.
610 53. Campo H, Murphy A, Yildiz S, Woodruff T, Cervelló I, Kim JJ. Microphysiological Modeling of
611 the Human Endometrium. Tissue Eng Part A. 2020;26(13-14):759-68. Epub 2020/04/30. doi:
612 10.1089/ten.tea.2020.0022. PubMed PMID: 32348708; PMCID: PMC7398432.
613 54. Xiao S, Coppeta JR, Rogers HB, Isenberg BC, Zhu J, Olalekan SA, McKinnon KE, Dokic D,
614 Rashedi AS, Haisenleder DJ, Malpani SS, Arnold-Murray CA, Chen K, Jiang M, Bai L, Nguyen
615 CT, Zhang J, Laronda MM, Hope TJ, Maniar KP, Pavone ME, Avram MJ, Sefton EC, Getsios S,
616 Burdette JE, Kim JJ, Borenstein JT, Woodruff TK. A microfluidic culture model of the human
617 reproductive tract and 28-day menstrual cycle. Nat Commun. 2017;8:14584. Epub 2017/03/30.
618 doi: 10.1038/ncomms14584. PubMed PMID: 28350383; PMCID: PMC5379057.
619 55. Banu SK, Lee J, Starzinski-Powitz A, Arosh JA. Gene expression profiles and functional
620 characterization of human immortalized endometriotic epithelial and stromal cells. Fertil Steril.
621 2008;90(4):972-87. Epub 2007/11/16. doi: 10.1016/j.fertnstert.2007.07.1358. PubMed PMID:
622 18001719.
623 56. Martin M. Cutadapt removes adapter sequences from high-throughput sequencing reads.
624 EMBnetjournal. 2011;17(1):pp-10.
625 57. Kim D, Langmead B, Salzberg SL. HISAT: A fast spliced aligner with low memory

626 requirements. Nat Methods. 2015;12(4):357-60. doi: 10.1038/nmeth.3317. PubMed PMID:
627 25751142; PMCID: PMC4655817.
628 58. Aken BL, Ayling S, Barrell D, Clarke L, Curwen V, Fairley S, Fernandez Banet J, Billis K,
629 Garcia Giron C, Hourlier T, Howe K, Kahari A, Kokocinski F, Martin FJ, Murphy DN, Nag R, Ruffier
630 M, Schuster M, Tang YA, Vogel JH, White S, Zadissa A, Flicek P, Searle SM. The Ensembl gene
631 annotation system. Database (Oxford). 2016;2016:1-19. Epub 2016/06/25. doi:
632 10.1093/database/baw093. PubMed PMID: 27337980; PMCID: PMC4919035.
633 59. Liao Y, Smyth GK, Shi W. featureCounts: an efficient general purpose program for assigning
634 sequence reads to genomic features. Bioinformatics. 2014;30(7):923-30. Epub 2013/11/15. doi:
635 10.1093/bioinformatics/btt656. PubMed PMID: 24227677.
636 60. Zhou X, Lindsay H, Robinson MD. Robustly detecting differential expression in RNA
637 sequencing data using observation weights. Nucleic Acids Res. 2014;42(11):e91. Epub
638 2014/04/23. doi: 10.1093/nar/gku310. PubMed PMID: 24753412; PMCID: PMC4066750.
639

ACKNOWLEDGEMENTS

The authors would like to sincerely thank all members of the Fazleabas laboratory, particularly Samantha Hrbek, Erin Vegter, and Ariadna Ochoa-Bernal, for their contributions to this project. We also thank Stephanie Celano for their assistance with live-cell imaging.

FUNDING

National Institutes of Health grant R01HD083273 (ATF)
National Institutes of Health grant R01HD099090 (ATF)
National Institutes of Health grant F32HD104478 (GWB)
Endometriosis Foundation of America (ATF)

AUTHOR CONTRIBUTIONS

Conceptualization: YS, GWB, ATF
Methodology: YS, GWB, RA, JK
Investigation: YS, GWB, NRJ
Visualization: YS, GWB, RA
Funding acquisition: GB, ATF
Project administration: ATF
Writing – original draft: YS, GB
Writing – review & editing: YS, GB, RA, JK, ATF

COMPETING INTERESTS

Authors declare that they have no competing interests.

FIGURES

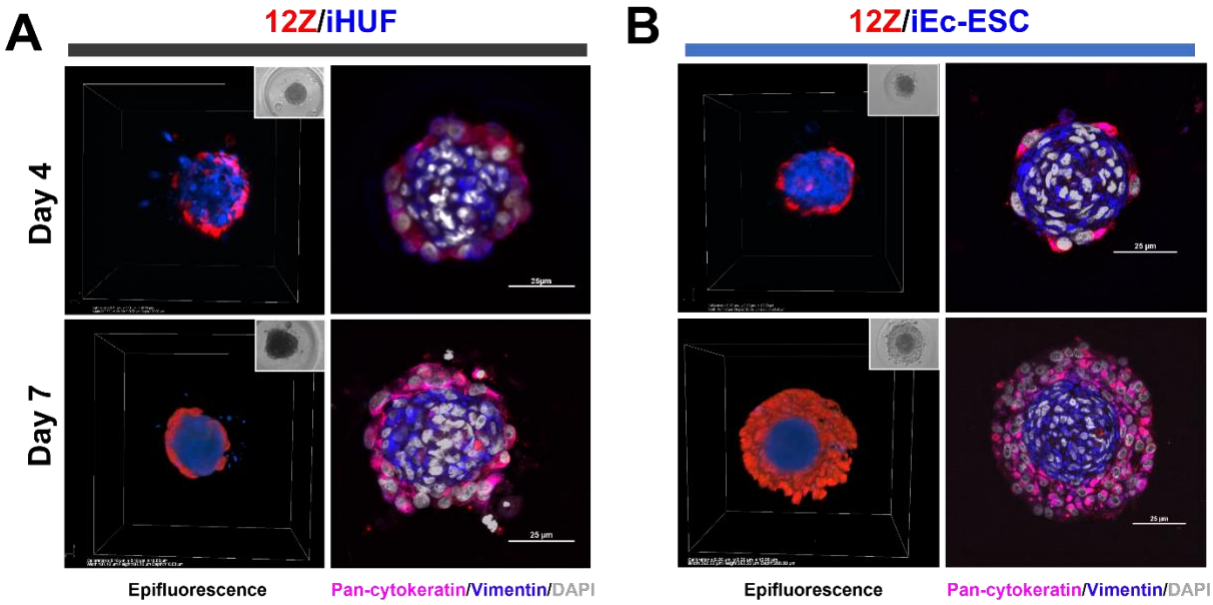

Fig 1. Organoid structure. Time course of organoids development derived from (A) 12Z-RFP/iHUF-Azurite Blue and (B) 12Z-RFP/iEc-ESC-Azurite Blue (endometriotic organoids, EO). The left panels are 3D views and inserts are phase contrast images. The right panels are immunofluorescent staining of vimentin (blue) and pan-cytokeratin (red). Scale bar = 25 µm.

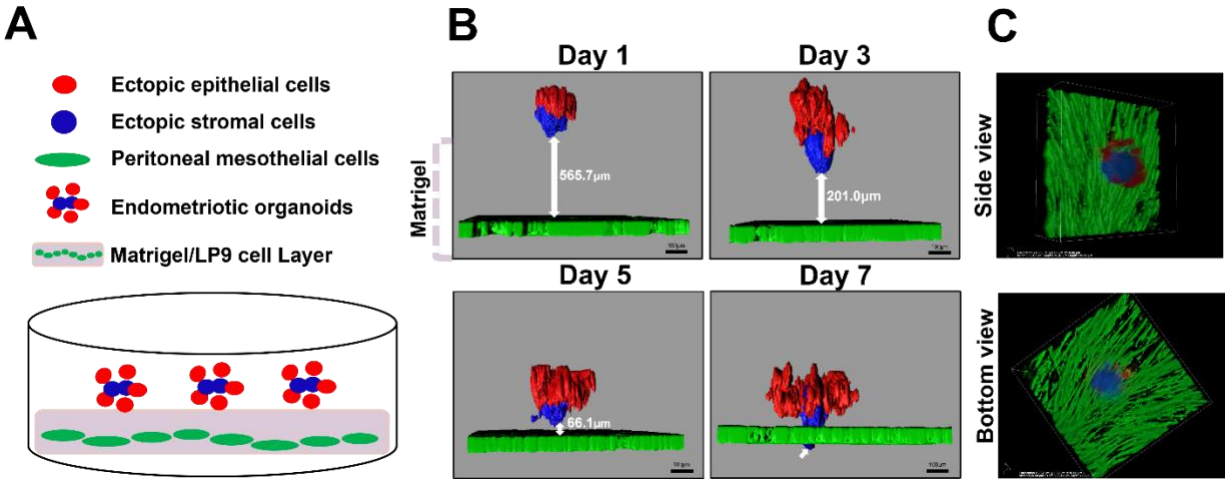

Fig 2. Organoid invasion model. Endometriotic organoids invade a 3D model of the peritoneum. (A) Schematic of the organoid invasion model. (B) Time course of organoid invasion quantified with Imaris image analysis software and relative to invasion into the mesothelial cell layer. Ectopic stromal cells were the leading edge of invasion through the LP9 cells. Note the penetration of organoids through the extracellular matrix and mesothelial cell layer in a time dependent manner. (C) Representative side view and bottom view of an EO invading the LP9 cells with stromal cells at the leading edge.

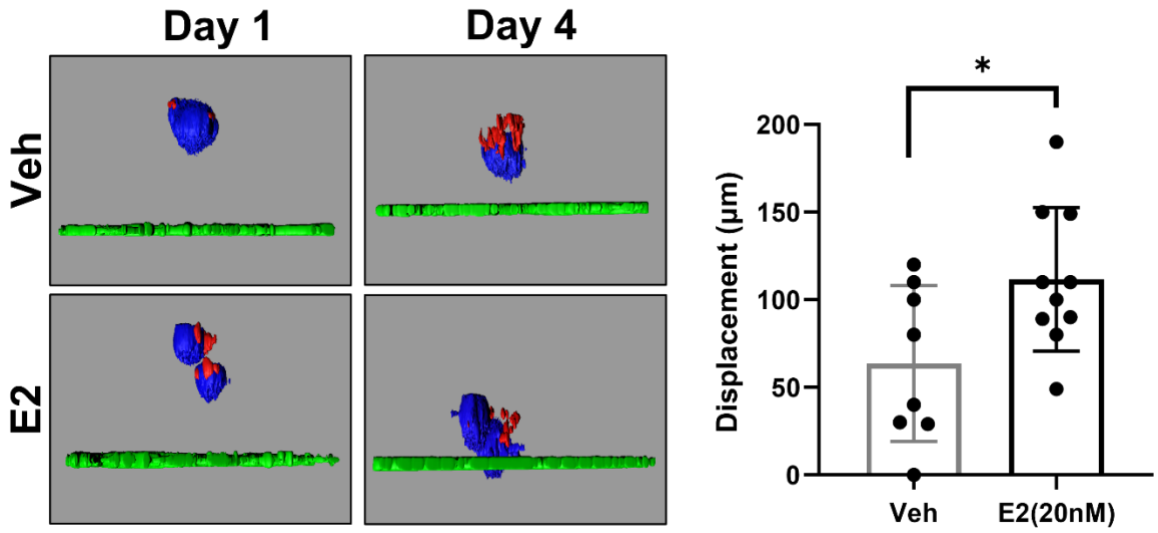

682

683

684 **Fig 3. Estrogen stimulates invasion of endometriotic organoids (EO).** Day 4 EO were seeded
685 on an LP9/Matrigel layer and treated with vehicle (ethanol, n=8) or estradiol (E2, 20nM, n=10) for
686 4 days. The EO were imaged on days 1 and 4 using fluorescent confocal microscopy and invasion,
687 relative to into the LP9 cell layer was quantified. Invasion was increased by 1.8-fold in the
688 presence of E2. *P<0.05

689

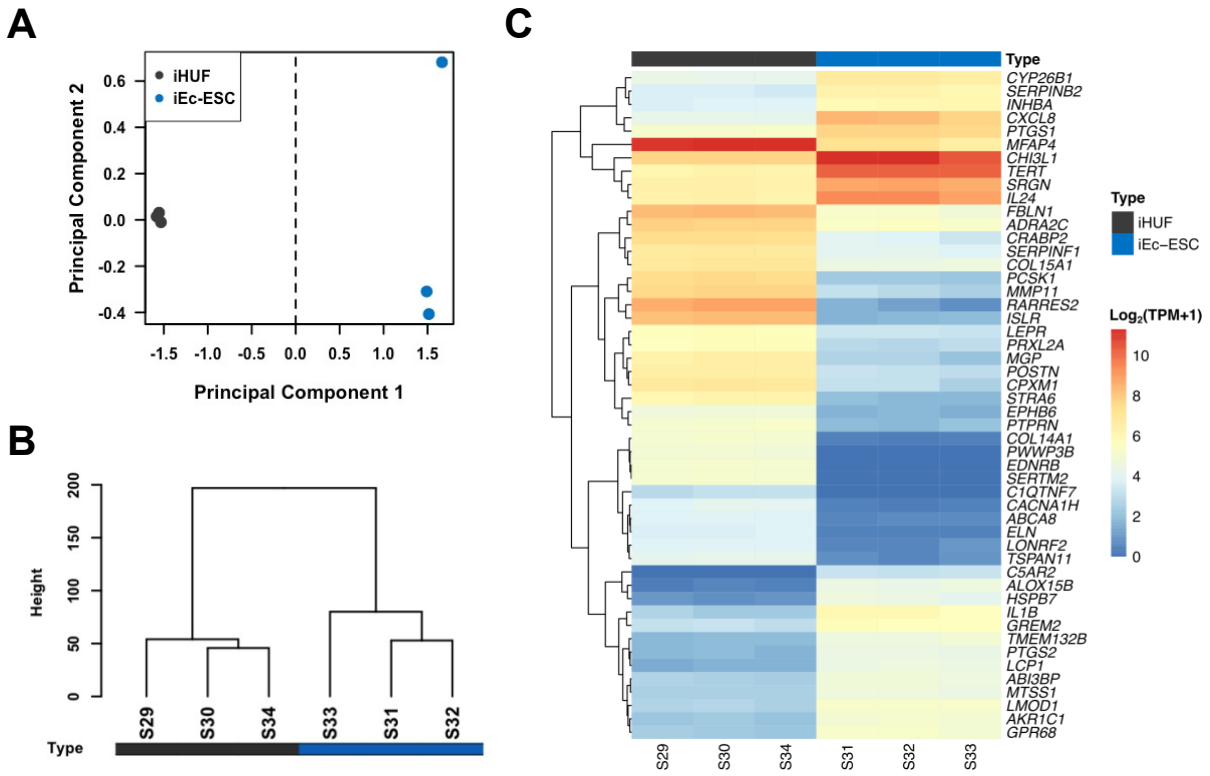

Fig 4. Stromal cell origin alters organoid gene expression. A) Principal component plot demonstrating transcriptome separation between iEc-ESC/12Z (EO) and iHUF/12Z organoids. B) Unsupervised hierarchical clustering dendrogram confirming separation of sample groups and C) a heat map of the top 50 differentially expressed genes with hierarchical gene clustering.

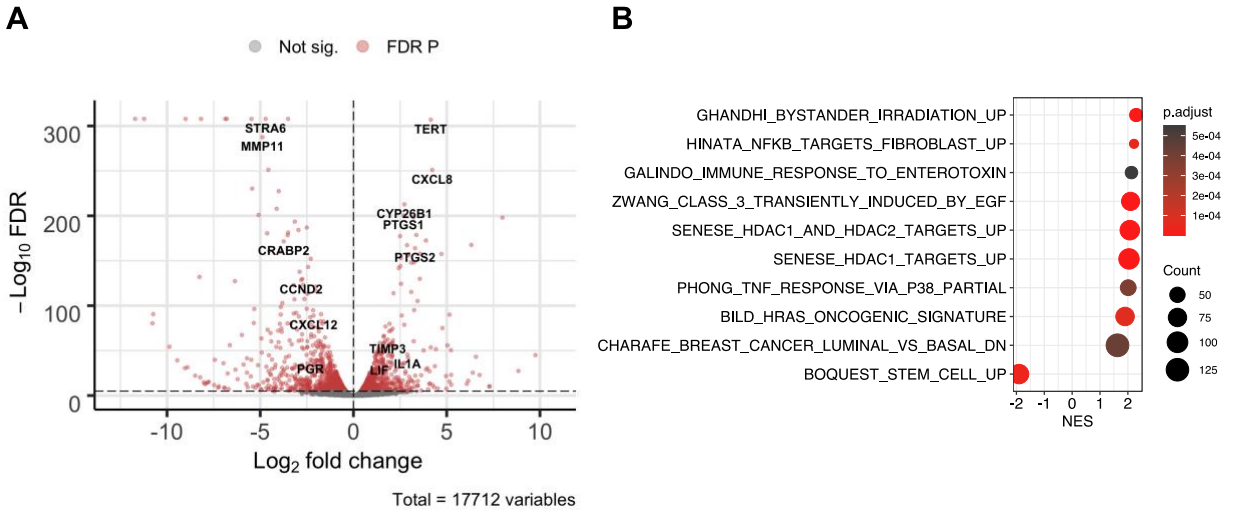

Fig 5. Transcriptome alterations in EO versus iHUF/12Z organoids. A) Volcano plot highlighting several top downregulated and upregulated genes in EO. B) The top MSigDB C2 enriched gene sets from human organoids. A positive normalized enrichment score (NES) indicates activation, or increased expression, of the gene set in EO.

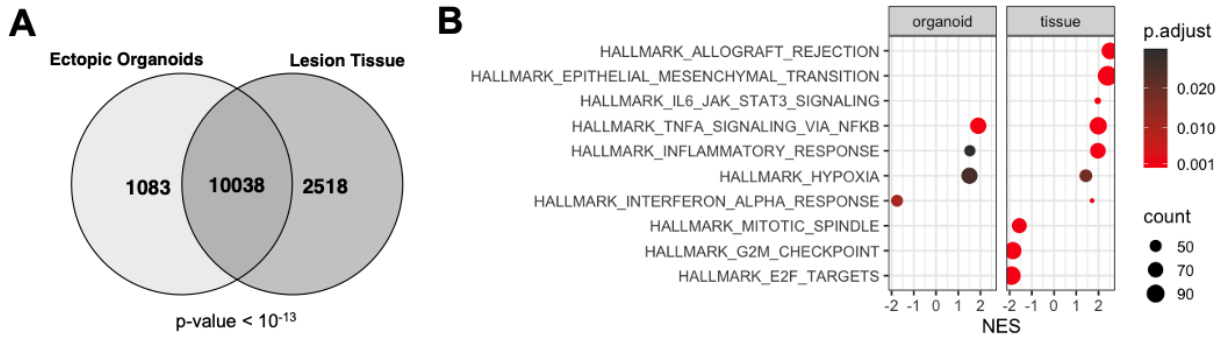

Fig 6. Endometriotic organoids (EO) and baboon lesion gene expression signatures are similar. A) The overlap of all expressed genes in EO and baboon lesions from spontaneous endometriosis is highly significant. B) Gene set enrichment analyses showed similar enrichment of NFKB, inflammatory response and hypoxia genes. NES= normalized enrichment score

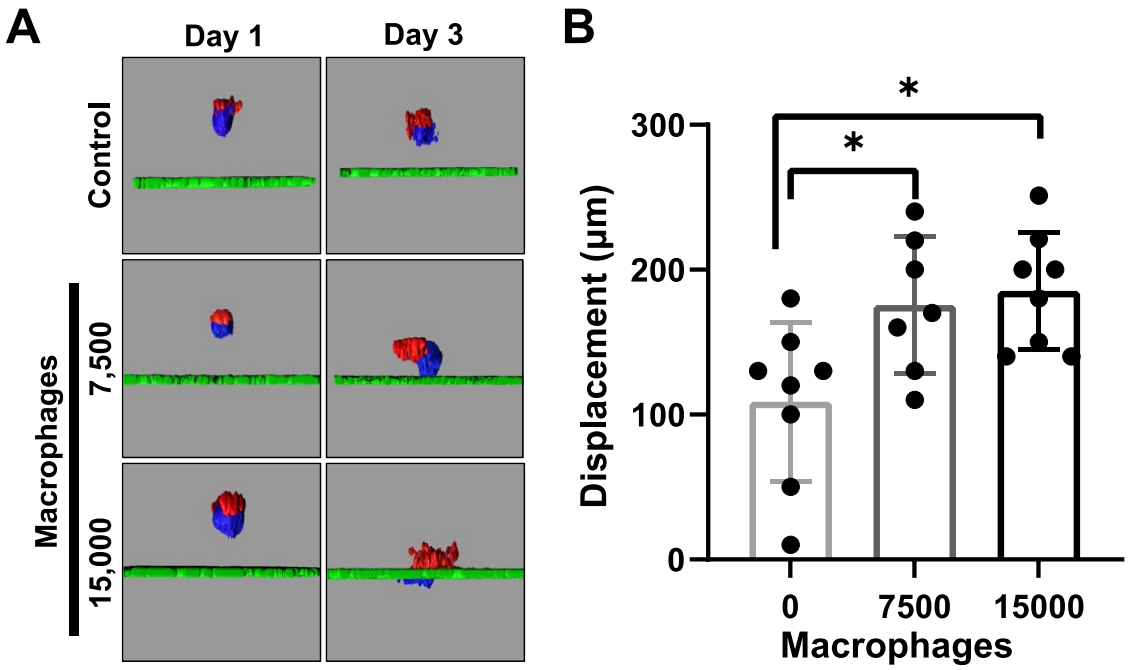

711
712

713 **Fig 7. Proinflammatory macrophages increase EO invasion.** (A) Day 4 EO were seeded on
714 an LP9/Matrigel layer and M1 macrophages (7,500 or 15,000) were added to the plates after 3h.
715 The EO were imaged on days 1 and 3 using fluorescent confocal microscopy and (B) invasion
716 relative to the LP9 cell layer, was quantified. Control n=8; M1 7,500 n=7; M1 15,000 n=8 *P<0.05

Table 1. Enrichment for immune-related genes in spontaneous endometriotic lesions. Top 10 enriched biological process gene ontology terms from genes expressed in baboon lesions and not human organoids.

PANTHER GO Slim (BP)	REFLIST	Input	Expected	Direction	Fold Enrichment	p-value	FDR
immune system process (GO:0002376)	258	128	44.67	+	2.87	3.56E-20	7.74E-18
immune response (GO:0006955)	163	90	28.22	+	3.19	9.35E-17	1.13E-14
cell surface receptor signaling pathway (GO:0007166)	544	177	94.18	+	1.88	1.44E-12	1.49E-10
signaling (GO:0023052)	1208	321	209.14	+	1.53	2.95E-12	2.92E-10
cell communication (GO:0007154)	1219	320	211.05	+	1.52	1.29E-11	1.08E-09
multicellular organismal process (GO:0032501)	682	204	118.08	+	1.73	1.45E-11	1.17E-09
signal transduction (GO:0007165)	1136	298	196.68	+	1.52	7.61E-11	4.73E-09
regulation of immune system process (GO:0002682)	127	64	21.99	+	2.91	7.87E-11	4.75E-09
leukocyte activation (GO:0045321)	57	40	9.87	+	4.05	2.04E-10	1.11E-08
positive regulation of immune system process (GO:0002684)	87	50	15.06	+	3.32	2.25E-10	1.19E-08